HPU2 Journal of Sciences:
Natural Sciences and Technology

Journal homepage: https://sj.hpu2.edu.vn

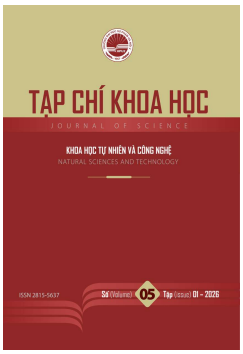

Article type: Research article

Constructing waveform of P, Q, R, S, and T waves in ECG signals for cardiovascular disease diagnosis

The-Lam Nguyen*, Quang-Huy Tran

Hanoi Pedagogical University 2, Phu Tho, Vietnam

Abstract

This study presents the development of an electrocardiogram (ECG) signal acquisition and analysis system based on Arduino hardware and a personal computer. The recorded ECG signals were processed in MATLAB to extract key diagnostic parameters, including sinus rhythm, the amplitude and width of the P, S, and T waves, as well as the slope of the ST segment. These features were subsequently transformed into Time-domain representations, enabling clinicians to simultaneously examine hundreds of cardiac cycles. By providing a comprehensive view of ECG variability, the proposed waveform effectively reduces the influence of artifacts caused by technical errors or transient physiological and emotional fluctuations. Consequently, the integration of s enhances diagnostic precision and reliability compared to conventional visual inspection methods currently used in clinical practice.

Keywords: electrocardiography (ECG), PQR waves, waveform, Arduino, MATLAB, cardiovascular disease diagnosis

1. Introduction

Electrocardiography (ECG) is a common, non-invasive clinical test that records the heart's electrical activity, widely used for diagnosis and monitoring of cardiovascular diseases [1]–[3]. In this method, electrodes are attached to the chest, arms, and legs to measure the electrical signals as they propagate through the heart, and the ECG signal is displayed as a waveform corresponding to each cardiac cycle [4], [5]. Within an ECG cycle, a wealth of pathological information is conveyed through the amplitude and width of component waves such as P, Q, R, S, and T [6]. The cycle duration and morphology of the ECG

* Corresponding author, E-mail: nguyenthelam@hpu2.edu.vn

https://doi.org/10.56764/hpu2.jos.2025.5.1.65-75

Received date: 18-9-2025 ; Revised date: 11-3-2026 ; Accepted date: 06-4-2026

provide critical diagnostic markers for conditions such as arrhythmias, myocardial ischemia and infarction, cardiac hypertrophy, pericarditis, and electrolyte imbalances [7]–[9].

Traditionally, clinical practice relies on visual inspection of ECG graphs, where physicians analyze the waves by measuring amplitudes and time intervals to assess cardiac electrical activity [10]. The heart rate and rhythm, reflected in ECG frequency, can indicate whether the heart is functioning regularly [11]. Alterations in the shape and size of the P, QRS, and T waves reveal structural or functional abnormalities in different cardiac chambers [12]. For example, disappearance of the P wave combined with irregular rhythm can indicate atrial fibrillation [13], while increased R-wave amplitude in limb leads and S-wave amplitude in chest leads suggests left ventricular hypertrophy (LVH) [14]. Similarly, a wide or notched P wave is linked to left atrial enlargement (LAE), whereas prolonged PR interval or widened QRS complex may indicate hyperkalemia [15]. Abnormalities in the QT interval are associated with electrolyte disturbances such as hypocalcemia [16]. Furthermore, the slope and morphology of the ST segment provide essential diagnostic insights: ST depression with inverted T waves suggests myocardial ischemia, while ST elevation across contiguous leads indicates myocardial infarction [17].

However, manual ECG interpretation has intrinsic limitations. Visual analysis requires considerable clinical experience and can be subjective, leading to inter-observer variability [18]. The human eye may not detect subtle waveform changes or rare abnormal beats when analyzing large volumes of ECG data, which risks missing early but clinically significant pathologies [19]. To overcome these challenges, recent studies have increasingly adopted automated ECG analysis methods, often enhanced with artificial intelligence (AI) and machine learning algorithms, which improve diagnostic accuracy and efficiency while supporting clinical decision-making [20]. Unlike conventional statistical methods where histograms only display frequency, the Waveform do more than represent instantaneous values (amplitude, position, etc.); they provide insights into the rate of change, peak amplitude, and fluctuation cycles of wave parameters in real-time. Most importantly, the spectral values are compared against standard clinical safety ranges in real-time.

Despite these advances, many existing studies primarily focus on pattern recognition of cardiac arrhythmias or large-scale classification tasks. Less attention has been paid to lightweight, real-time ECG acquisition and analysis systems that can be deployed in low-resource or educational settings. Furthermore, developing an integrated framework that not only acquires ECG signals but also performs fundamental spectral decomposition of cardiac waves (e.g., P-wave amplitude, R-wave height, ST slope) is essential for both clinical research and training applications. Our study addresses this gap by designing a low-cost ECG measurement system using AD8232 and Arduino, combined with MATLAB-based signal processing for real-time visualization and spectral feature extraction. This approach is expected to provide a practical tool for both clinical support and biomedical engineering education, highlighting the necessity and timeliness of our research.

2. Design of the ECG Signal Measurement System

To construct the Waveform, we will identify the positions (timing) and measure the values (amplitude, width, slope, etc.) of the waves (P, Q, R, S, T, etc.) within each recorded ECG signal cycle, then represent their variations (amplitude, width, position, etc.) over real-time. The block diagram of the ECG measurement system is connected as shown in Figure 1.

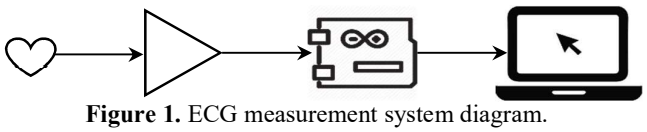

Figure 1. ECG measurement system diagram.

Electrodes: These are small metal pads or adhesive patches placed on the patient's skin at specific locations on the arms, legs, and chest. Their function is to pick up the electrical signals generated by the heart.

Amplifier: Because the electrical signals produced by the heart are very small, an amplifier is needed to boost the signal's amplitude so the machine can record it. In this report, we use the AD8232 module (Figure 2).

Figure 2. AD8232 Sensor Module.

Figure 3. Arduino Uno Module.

Signal Processor/ADC (Analog-to-Digital Converter): This component converts the analog signal into a digital signal and inputs it into the PC. In this report, we use the analog ports of Arduino (Figure 3).

*ECG Display***:** The display is a Figure window in MATLAB, showing the electrocardiogram in real time.

Signal Processing to Find Wave-waveform: The ECG signal is processed by MATLAB through a program for storage and analysis. The waveforms are also output as graphs, such as P-wave amplitude, P-wave width, R-wave amplitude, ST segment slope, and more.

To receive ECG signals from the sensor and transmit them to the computer, Arduino was programmed to meet the connection requirements. The connection program was written in C++ language using the IDE application. This program is then compiled into binary code and uploaded to the microcontroller chip's memory on the Arduino. After conversion to a digital signal, the signal is connected to the computer via a USB port. MATLAB then reads the signal from the USB port and reconstructs it as a graph.

The circuit diagram of connection is shown in Figure 4 and the program to connect the AD8232 module with Arduino is written as follows. Whereas, the Analog-to-Digital Converter (ADC) resolution used on our device is 10-bit (the default setting for Arduino) and the reference voltage for the Arduino is set at the standard 5V.

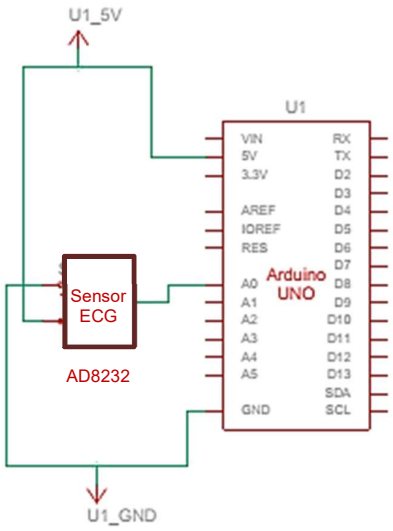

Figure 4. The circuit diagram of the ECG measurement system.

The sampling frequency is determined by the time interval (period) required to measure an ECG value over time. In this study, we programmed this interval to be 5 ms, corresponding to a sampling frequency of 200 Hz. The code of connection is written in C as follows.

```
// Define A0 as Analog input
#define ECG_IN A0
float voltage = 0.0;
float max_voltage = 5.0;
int ADC_value = 0;

void setup(){
  Serial.begin(9600);
  Serial.println("ECG signal");
}

void loop(){
  // Read Analog ECG
  adc_value = analogRead(ECG_IN);

  // Convert ADC_value  to float
 voltage  = (ADC_value * max_voltage) / 1024.0;

  // Print voltage to Serial Monitor
 Serial.print("ECG Voltage = ");
 Serial.println(voltage, 2);
 delay(5);
}
```

To receive the ECG signal from Arduino, we use MATLAB to open the computer's COM port, which is connected to the Arduino. This allows us to receive the ECG signals and plot them on MATLAB's graphical window, displaying 100 signals per frame. The MATLAB program is written simply as follows.

```
% Open COM3
close all; clear all; clf;
```

```
s = serial('COM3','BaudRate',9600);
fopen(s);
disp('Press CTRL + C to Stop');
%Plot data
i = 0;
while (1)
   i = i + 1;
   ECG(i) = fscanf(s,'%d');
   plot(ECG);
   pause(0.001);
   if i > 100
      i = 1;
      clf;
   end;
end;
fclose(s);
```

3. Processing ECG Signal for Constructing Waveform

In our system, approximately 18 points define a cycle, which will contain enough P, Q, R, S, and T waves. Since the start time of signal acquisition is quite random, determining the exact positions of these waves within a cycle is rather complex.

First, we identify the positions of the extrema as the locations of unidentified waves within an ECG cycle. If we consider the ECG signal as a discrete function of time, F(t), then the identification of these extrema positions is performed by solving the discrete equation F′(t) = 0 using numerical methods. The positions (time) of these extrema will be organized into a vector called the extrema position vector (Tmax). The corresponding amplitudes of these extrema (wave peaks) will be stored in the extrema amplitude vector Fmax).

Looking at the ECG signal graph, we can see that the R-wave has the highest amplitude and is significantly different from the amplitudes of the other waves. This makes it a good indicator for identifying the R-wave's position within an ECG cycle and its index within the Tmax vector.

If we divide the cycle T of an ECG signal into N segments (in this paper, we choose N = 17), with each segment defined as follows:

$$\Delta t = \frac{T}{N} \tag{1}$$

We have, $t_i = t_0 + i\Delta t$, where t_0 is the initial measurement time determined from real-time, and i = 1… N + 1 are integers. At that time, the ECG wave amplitudes are recorded as values $F_i = SERIAL(t_i)$, where SERIAL(t) is the value measured from the USB port via the sensor ECG and Arduino. The first-order numerical derivative is approximated as:

$$F_i' = \frac{F_{i+1} - F_i}{\Delta t} = \frac{\Delta F_i}{\Delta t} \tag{2}$$

Where i = 1 … N, by the halving method.

For i = 1 to N

$t_i = t_0 + i\Delta t$

$F_i = SERIAL(t_i)$

$k = 1$

IF $(F_i' * F_{i+1}' < 0)$ then

$$t_{\max(k)} = \frac{t_i + t_{i+1}}{2}$$

$$F_{\max(k)} = \frac{F_i + F_{i+1}}{2}$$

END

$k = k + 1$

END

Using the bisection method, we found the extreme values (peaks of the waves) as an extreme amplitude vector Fmax and the positions (time) of these extremes as an extreme position vector Tmax. Also using this algorithm, we can easily find the largest value in the extreme amplitude vector (the R-wave peak). Thus, the extreme position vector Tmax and the extreme amplitude vector Fmax have been determined. We can write these two vectors in matrix form.

$$T_{max} = (t_P \quad t_Q \quad t_R \quad t_S \quad t_T) \tag{3}$$

$$F_{max} = (F_P \quad F_Q \quad F_R \quad F_S \quad F_T) \tag{4}$$

Each measurement has an undefined starting time, so the amplitude and position of the R-wave are determined as follows.

$$F_R = Max(F_{max}) = F_{max}(k)$$

$$t_R = T_{max}(k)$$

If k is called as the index or position of F_R or t_R in the vector T_{max}, then the positions of the other waves like S, T, P, and Q are determined as follows:

The amplitude and position of the S-wave.

$F_S = F_{max}(k + 1)$
$t_S = T_{max}(k + 1)$
IF $(k + 1 > 5)$ then
$k + 1 = k + 1 - 5$
$F_S = F_{max}(k - 4)$
$t_S = T_{max}(k - 4)$
END

The amplitude and position of the T-wave

$F_S = F_{max}(k + 2)$
$t_S = T_{max}(k + 2)$
IF $(k + 2 > 5)$then
$k + 2 = k + 2 - 5$
$F_S = F_{max}(k - 3)$
$t_S = T_{max}(k - 3)$
END

The amplitude and position of the Q-wave

$F_Q = F_{max}(k - 1)$
$t_Q = T_{max}(k - 1)$
IF $(k - 1 < 0)$ then
$k - 1 = k - 1 + 5$
$F_Q = F_{max}(k + 4)$
$t_Q = T_{max}(k + 4)$
END

The amplitude and position of the P-wave

$F_P = F_{max}(k - 2)$

$t_P = T_{max}(k-2)$
IF $(k-2<0)$ then
$k-2 = k-2+5$
$F_P = F_{max}(k+3)$
$t_P = T_{max}(k+3)$
END

After each cycle, the time vector t and amplitude vector F are recorded to determine the width of the P, Q, R, S, and T waves.

With the wave height error $\varepsilon = 10^{-2}$ (%), the width of the P-wave can be determined by the following algorithm.

FOR i = 1 to N + 1
$t_i = t_0 + i\Delta t$
$F_i = SERIAL(t_i)$
$w_P = 0$
IF $(t_i > t_P)$ & $(|F_i| > \varepsilon)$ then
$w_P = w_P + 1$
END
$w_P = 2 * w_P * \Delta t$
END

This algorithm is applied similarly to find the width of the Q, R, S, and T waves.

The slope of the ST segment is determined by the angle α_{ST} as shown in Figure 5, where

$$\tan(\alpha_{ST}) = \frac{F_T - F_S}{t_T - t_S} \tag{5}$$

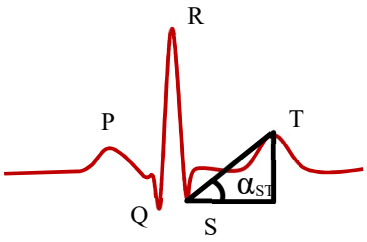

Figure 5. The slope of the ST segment is calculated using the angle α_{ST}.

After m ECG cycles, we obtain the matrices.

$$T_{max} = \begin{pmatrix} t_P^{(1)} & t_Q^{(1)} & t_R^{(1)} & t_S^{(1)} & t_T^{(1)} \\ t_P^{(2)} & t_Q^{(2)} & t_R^{(2)} & t_S^{(2)} & t_T^{(2)} \\ & & \cdots & & \\ & & \cdots & & \\ t_P^{(m)} & t_Q^{(m)} & t_R^{(m)} & t_S^{(m)} & t_T^{(m)} \end{pmatrix} \tag{6}$$

and

$$F_{max} = \begin{pmatrix} F_P^{(1)} & F_Q^{(1)} & F_R^{(1)} & F_S^{(1)} & F_T^{(1)} \\ F_P^{(2)} & F_Q^{(2)} & F_R^{(2)} & F_S^{(2)} & F_T^{(2)} \\ & & \cdots & & \\ & & \cdots & & \\ F_P^{(m)} & F_Q^{(m)} & F_R^{(m)} & F_S^{(m)} & F_T^{(m)} \end{pmatrix} \tag{7}$$

From these matrices, we can also find the column matrices for the widths of the waves W_P, W_Q, W_R, W_S, W_T and α_{ST} for the slope of the ST segment.

$$W_P = \begin{pmatrix} w_P^{(1)} \\ w_P^{(2)} \\ \cdots \\ \cdots \\ w_P^{(m)} \end{pmatrix}; W_Q = \begin{pmatrix} w_Q^{(1)} \\ w_Q^{(2)} \\ \cdots \\ \cdots \\ w_Q^{(m)} \end{pmatrix}; W_R = \begin{pmatrix} w_R^{(1)} \\ w_R^{(2)} \\ \cdots \\ \cdots \\ w_R^{(m)} \end{pmatrix} \cdots\cdots \alpha_{ST} = \begin{pmatrix} \alpha_{ST}^{(1)} \\ \alpha_{ST}^{(2)} \\ \cdots \\ \cdots \\ \alpha_{ST}^{(m)} \end{pmatrix} \quad (8)$$

By collecting the values in the first column of the Fmax matrices, we were able to plot the *amplitude spectrum* of the P-wave. The *amplitude waveform* of the Q, R, S, and T waves were similarly constructed from the remaining columns of the Fmax matrix. The *width waveform* of the P, Q, R, S, T waves and the *spectrum of the ST segment slope* were also determined using the column matrices (8).

Sinus rhythm can also be calculated using the Tmax position matrix.

$$f_{ECG} = \frac{60}{T_{ECG}} \quad \text{(rhythm/minute)} \quad (9)$$

Where T_{ECG} is the period of an ECG signal measured in seconds, for the *i*-th cycle, it is calculated as follow

$$T_{ECG}^{(i)} = t_R^{(i+1)} - t_R^{(i)}$$

The *sinus rhythm spectrum* can be constructed from the elements of the vector f_{ECG}

$$f_{ECG} = (f_{ECG}^{(1)} \; f_{ECG}^{(2)} \quad \cdots \quad f_{ECG}^{(N-1)}) \quad (10)$$

Unlike the Pan–Tompkins algorithm, which relies on signal slope (first-order derivative) to detect the R-wave position and subsequently identify other waveforms, our algorithm first identifies the local extrema of all waves within an ECG cycle. By searching for the maximum peak (R-wave) followed by the minimum peak (S-wave), the position and amplitude of both R and S waves are determined with high precision and zero ambiguity. Consequently, it can be concluded that our algorithm offers superior accuracy and stability

To demonstrate an educational prototype for the construction and application of wave spectra (P, Q, R, S, T) in diagnosing cardiovascular diseases. Our experiment was conducted for the unipolar limb lead I (negative electrode on the right arm, positive electrode on the left arm) as shown in Figure 6.

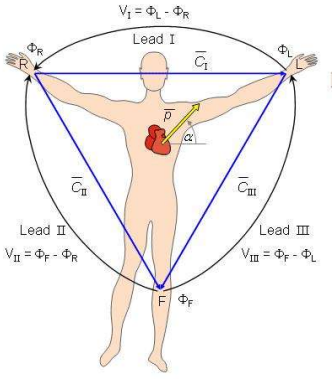

Figure 6. The unipolar limb leads.

The waveforms obtained are shown in the following figures from 7 to 12. The ECG voltage is plotted on the default scale of the Arduino's analog input, which consists of integers from 0-1023. To convert these digital values into clinical ECG voltages, the following formula can be applied

$$V_{clin} = \frac{V_{in} \times 5000}{1024} \text{ (mV)} \quad (11)$$

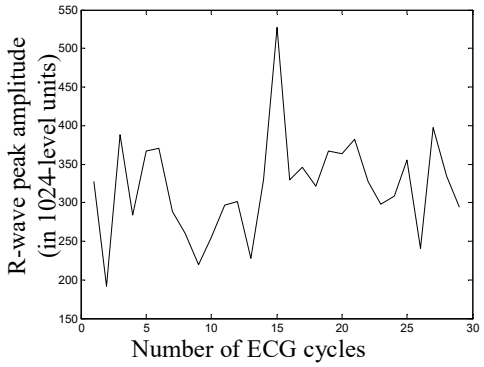

Figure 7. The R-wave peak amplitude waveform.

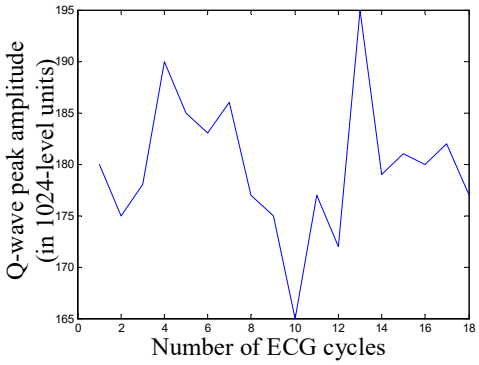

Figure 8. The Q-wave peak amplitude waveform.

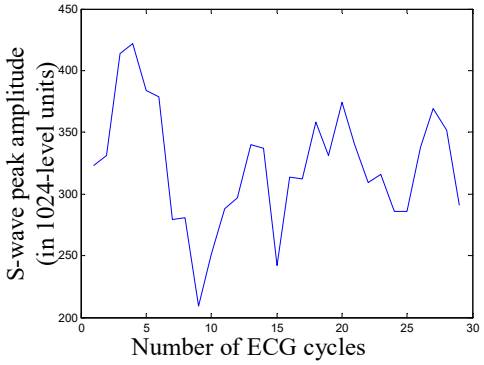

Figure 9. The S-wave peak amplitude waveform.

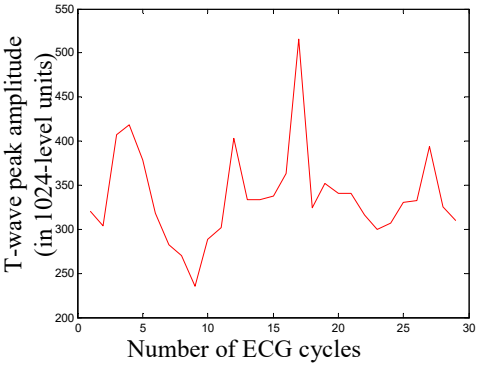

Figure 10. The T-wave peak amplitude waveform.

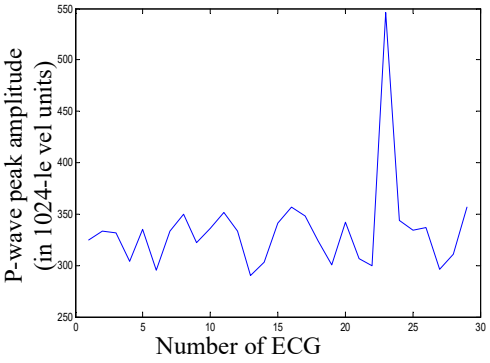

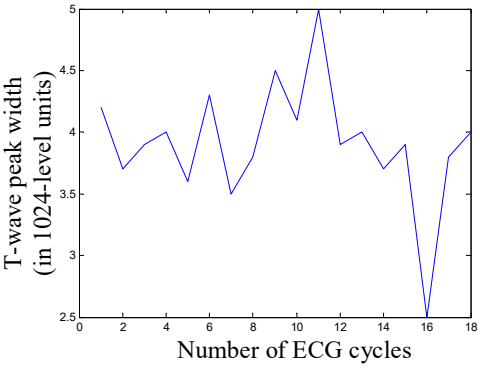

Figure 11. The P-wave peak amplitude waveform.

Figure 12. The T-wave peak width waveform.

4. Conclusions

In this paper, we successfully constructed an electrical circuit to connect an ECG sensor to a personal computer via an ADC converter using an Arduino board. The code for Arduino was written in C using the IDE software. The ECG signal was fully displayed on the screen in real-time. We utilized MATLAB as a tool for signal processing and display. Within the scope of this paper, only one unipolar limb lead was implemented, and we successfully constructed the amplitude and width waveform for the P, Q, R, S, and T waves for this lead. The slope spectrum of the ST segment and the sinus rhythm spectrum for this lead were also obtained. By observing the waveform, physicians can easily identify abnormal values that need to be excluded and reliable, stable values that can be used for diagnosis. The safe ranges (such as amplitude, width, slope, etc.) for each type of lead should be strictly referenced according to current medical literature. The standardization of the signal with standard medical ECG signals for various subjects (men, women, elderly, children, etc.) was not performed in this paper.

The construction of Waveform for other leads (12-lead ECG) can be performed in an entirely analogous manner. In practice, the technician or physician simply needs to reposition the electrodes on the patient's body. Naturally, the spectral profiles for different leads will be compared against the clinical reference database corresponding to each specific lead

References

[1] J. Pan and W. J. Tompkins, "A real-time QRS detection algorithm," *IEEE Trans. Biomed. Eng.*, vol. BME-32, no. 3, pp. 230–236, Mar. 1985, doi: 10.1109/TBME.1985.325532.

[2] P. Laguna, R. G. Mark, A. Goldberg, and G. B. Moody, "A database for evaluation of algorithms for measurement of QT and other waveform intervals in the ECG," *Comput. Cardiol.*, vol. 24, pp. 673–676, 1997, doi: 10.1109/CIC.1997.648140.

[3] J. P. Martínez, R. Almeida, S. Olmos, A. P. Rocha, and P. Laguna, "A wavelet-based ECG delineator: Evaluation on standard databases," *IEEE Trans. Biomed. Eng.*, vol. 51, no. 4, pp. 570–581, Apr. 2004, doi: 10.1109/TBME.2003.821031.

[4] P. De Chazal, M. O'Dwyer, and R. B. Reilly, "Automatic classification of heartbeats using ECG morphology and heartbeat interval features," *IEEE Trans. Biomed. Eng.*, vol. 51, no. 7, pp. 1196–1206, Jul. 2004, doi: 10.1109/TBME.2004.827359.

[5] G. B. Moody and R. G. Mark, "The impact of the MIT-BIH arrhythmia database," *IEEE Eng. Med. Biol. Mag.*, vol. 20, no. 3, pp. 45–50, May–Jun. 2001, doi: 10.1109/51.932724.

[6] C. Ye, B. V. Kumar, and M. T. Coimbra, "Heartbeat classification using morphological and dynamic features of ECG signals," *IEEE Trans. Biomed. Eng.*, vol. 59, no. 10, pp. 2930–2941, Oct. 2012, doi: 10.1109/TBME.2012.2213253.

[7] M. Llamedo and J. P. Martínez, "Heartbeat classification using feature selection driven by database generalization criteria," *IEEE Trans. Biomed. Eng.*, vol. 58, no. 3, pp. 616–625, Mar. 2011, doi: 10.1109/TBME.2010.2068048.

[8] J. Bergquist, et al., "Body surface potential mapping: contemporary applications and future perspectives," *Hearts*, vol. 2, no. 4, pp. 514–542, 2021, doi: 10.3390/hearts2040040.

[9] Z. F. M. Apandi, N. Ahmad, H. S. A. Wahab, and N. Ahmad, "An analysis of the effects of noisy electrocardiogram signal on heartbeat detection performance," *Bioengineering*, vol. 7, no. 2, p. 53, May 2020, doi: 10.3390/bioengineering7020053.

[10] A. L. Goldberger et al., "PhysioBank, PhysioToolkit, and PhysioNet: Components of a new research resource for complex physiologic signals," *Circulation*, vol. 101, no. 23, pp. e215–e220, Jun. 2000, doi: 10.1161/01.CIR.101.23.e215.

[11] P. S. Hamilton, "Open source ECG analysis," *Comput. Cardiol.*, vol. 29, pp. 101–104, 2002, doi:

10.1109/CIC.2002.1166717.

[12] R. Acharya, J. Suri, J. Spaan, and S. Krishnan, Eds., *Advances in Cardiac Signal Processing*. Berlin, Germany: Springer, 2007, doi: 10.1007/978-3-540-36675-1.

[13] J. Sörnmo and L. Sörnmo, *Bioelectrical Signal Processing in Cardiac and Neurological Applications*. Amsterdam, The Netherlands: Academic Press, 2005, doi: 10.1016/B978-012437552-9/50007-6.

[14] F. Zhou and D. Fang, "Multimodal ECG heartbeat classification method based on a convolutional neural network embedded with FCA," *Sci. Rep*., vol. 14, no. 1, p. 8804, 2024, doi: 10.1038/s41598-024-59311-0.

[15] Y. Lecun, Y. Bengio, and G. Hinton, "Deep learning," *Nature*, vol. 521, pp. 436–444, May 2015, doi: 10.1038/nature14539.

[16] U. R. Acharya et al., "Automated identification of shockable and non-shockable life-threatening ventricular arrhythmias using convolutional neural network," *Future Gener. Comput. Syst.*, vol. 79, pp. 952–959, Feb. 2018, doi: 10.1016/j.future.2017.08.039.

[17] Í. F. Di Paolo, A. R. G. Castro, "Intra- and Interpatient ECG Heartbeat Classification Based on Multimodal Convolutional Neural Networks with an Adaptive Attention Mechanism," *Applied Sciences*, vol. 14, no. 20, 9307, 2024, doi: 10.3390/app14209307.

[18] K. Faust, U. R. Acharya, H. Adeli, and D. J. Adeli, "Wavelet-based EEG processing for computer-aided seizure detection and epilepsy diagnosis," *Seizure*, vol. 26, pp. 56–64, Feb. 2015, doi: 10.1016/j.seizure.2015.01.012.

[19] A. Hannun et al., "Cardiologist-level arrhythmia detection and classification in ambulatory electrocardiograms using a deep neural network," *Nat. Med.*, vol. 25, pp. 65–69, Jan. 2019, doi: 10.1038/s41591-018-0268-3.

[20] C. Zhang, W. Chen, H. Chen, "Denoising for ECG signals based on VMD and RLS," *Journal of Measurements in Engineering*, vol. 13, no. 1, pp. 185-204, Mar. 2025, doi: 10.21595/jme.2025.24577.